

Sensitivity of sea-to-air CO₂ flux to ecosystem parameters from an adjoint model

J. F. Tjiputra^{1,2} and A. M. E. Winguth³

¹Department of Atmospheric Oceanic and Space Sciences, University of Wisconsin, Madison, Wisconsin, USA

²now at: Bjerknes Centre for Climate Research, University of Bergen, Bergen, Norway

³Department of Earth and Environmental Sciences, University of Texas, Arlington, Texas, USA

Received: 5 April 2007 – Published in Biogeosciences Discuss.: 27 April 2007

Revised: 20 December 2007 – Accepted: 4 March 2008 – Published: 25 April 2008

Abstract. An adjoint model is applied to examine the biophysical factors that control surface pCO₂ in different ocean regions. In the tropical Atlantic and Indian Oceans, the annual cycle of pCO₂ in the model is highly dominated by temperature variability, whereas both the temperature and dissolved inorganic carbon (DIC) are important in the tropical Pacific. In the high-latitude North Atlantic and Southern Oceans, DIC variability mainly drives the annual cycle of surface pCO₂. Phosphate addition significantly increases the carbon uptake in the tropical and subtropical regions, whereas nitrate addition increases the carbon uptake in the subarctic Pacific Ocean. The carbon uptake is also sensitive to changes in the physiological rate parameters in the ecosystem model in the equatorial Pacific, North Pacific, North Atlantic, and the Southern Ocean. Zooplankton grazing plays a major role in carbon exchange, especially in the HNLC regions. The grazing parameter regulates the phytoplankton biomass at the surface, thus controlling the biological production and the carbon uptake by photosynthesis. In the oligotrophic subtropical regions, the sea-to-air CO₂ flux is sensitive to changes in the phytoplankton exudation rate by altering the flux of regenerated nutrients essential for photosynthesis.

et al., 2002). The carbon uptake by the ocean is regulated by a combination of physical, chemical, and biological dynamics. Understanding and identifying these regional and temporal physical as well as biogeochemical processes are critical for predicting the response of global carbon cycle to the anthropogenic loading of atmospheric CO₂ in the future. Due to the non-linear characteristics of the marine carbon cycle dynamics, it can be problematic to determine whether biological or physical processes are the dominant controls of the sea-to-air CO₂ flux (Oschlies and Köhler, 2004). Different methods have been explored to assess the magnitude of these controlling processes. An empirical study by Takahashi et al. (2002) used ocean pCO₂ observations to analyze its seasonal and geographical variability due to sea surface temperature (SST) and biological activity. Völker et al. (2002) applied a box model to estimate how the atmospheric carbon uptake would likely be altered by the changes in future physical forcing and heat fluxes. Model studies with three-dimensional, marine carbon cycle models (e.g. Le Quéré et al., 2000; McKinley et al., 2004; Wetzel, 2004) used the approximation of the linearized pCO₂ formulation to estimate the different tendencies due to dissolved inorganic carbon, temperature, alkalinity, and salinity based on the Takahashi et al. (1993) method. However, these model studies mainly focused on interannual-to-decadal timescales rather than on seasonal variability. Here we have used an adjoint model to investigate the relative importance of different biophysical processes in determining the seasonal variability of surface pCO₂. In addition, we explored the physical and biogeochemical factors controlling the simulated seasonal variability of DIC.

Both means by which carbon is taken up, redistributed, and lost from the ocean, i.e., the solubility and biological pumps (Volk and Hoffert, 1985), are likely to be altered in the future. The strength of solubility pump will be reduced by the warming of SST (Weiss, 1974), thereby reducing uptake

1 Introduction

The anthropogenic climate perturbations during the past century have altered global biogeochemistry and will have long-term influence on the earth radiative forcing. These changes together with complex feedback processes may alter the strength and rate of carbon uptake by the ocean (Falkowski



Correspondence to: J. F. Tjiputra
(jerry.tjiputra@bjerknes.uib.no)

of atmospheric CO₂ (Maier-Reimer et al., 1996; Sarmiento et al., 1998; Matear and Hirst, 1999; Plattner et al., 2001; Mikolajewicz et al., 2007). Moreover, future changes in the ocean circulation will also influence ocean ecology and biogeochemistry, which can feedback on the circulation (Manizza et al., 2005; Wetzel et al., 2005; Winguth et al., 2005). Future climate-induced changes in ecosystem dynamics can include shoaling of mixed layer depth due to increase of stratification (Denman and Pena, 2002; Wrona et al., 2006), increase in aeolian iron flux (Bopp et al., 2003; Parekh et al., 2006), as well as changes in planktonic physiological rates (Denman and Pena, 2002; Le Quéré et al., 2005). The sensitivity of sea-to-air CO₂ flux to regional perturbations of surface iron concentration has been explored by several studies (Sarmiento and Orr, 1991; Bopp et al., 2003; Gnanadesikan et al., 2003; Zeebe and Archer, 2005; Aumont and Bopp, 2006; Dutkiewicz et al., 2006; Parekh et al., 2006). Except for Dutkiewicz et al. (2006), these sensitivity experiments were made with forward model perturbations. Here we applied an adjoint model to investigate the sensitivity of sea-to-air CO₂ flux to changes in nutrient concentration and physiological parameters in the marine ecosystem model. Relative to the multiple approximated sensitivities from a forward, finite-differences approach, the adjoint method allows us to simultaneously compute the exact sensitivity of the regional (grid-scale) carbon uptake to various biogeochemical tracers and parameters such as surface nutrient concentration, phytoplankton growth, phytoplankton exudation, zooplankton grazing, and zooplankton excretion rates.

The main objectives of this study are (1) to apply an adjoint model to investigate the dominant seasonal and regional biophysical factors that regulate surface pCO₂ variability and (2) to quantitatively estimate the sensitivity of the sea-to-air CO₂ flux to changes in regional nutrient concentrations and marine ecosystem parameters by mapping the grid-scale sensitivity distributions. This estimated sensitivity analysis was based on the effects of long-term (i.e., ten-year) nutrient and ecosystem parameter perturbations on atmospheric carbon uptake by the ocean.

2 Methods

2.1 Models

We used the off-line Hamburg Ocean Carbon Cycle (HAMOCC5) model, which is based on work by Maier-Reimer (1993), Six and Maier-Reimer (1996), Aumont et al. (2003), and Gehlen et al. (2003). The HAMOCC5 model was integrated offline for 10 000 years to reach a steady state using a climatological repeated annual cycle of physical forcing generated by the Large Scale Geostrophic (LSG, Maier-Reimer et al., 1993) ocean general circulation model. The model has an approximately 3.5° × 3.5° horizontal resolution and 22 vertical layers with thicknesses varying from 50 m at

the surface to 700 m in the deepest layer. Its components include an intermediate NPZD-type ecosystem model (Six and Maier-Reimer, 1996; Aumont et al. 2003), marine carbon chemistry (Heinze et al., 1999), a 12-layer sediment model, a diffusive atmosphere layer, sea-to-air gas exchange bulk formulation (Wanninkhof, 1992), and a parameterization of iron-limited particulate organic carbon export (Howard et al., 2006). The ecosystem model also accounts for atmospheric nitrogen fixation by cyanobacteria, parameterized as a relaxation of surface-layer deviation of the N:P ratio to the stoichiometric Redfield ratio (Maier-Reimer et al., 2005). The geochemical tracers in the model are advected with a time step of one month, while a shorter time step of three days is used in the euphotic zone (i.e., in the upper two layers of the model) to resolve ecosystem and sea-to-air gas exchange processes.

Here, the sea-to-air CO₂ flux formulation is based on the study by Wanninkhof (1992)

$$F_{\text{CO}_2} = k(p\text{CO}_{2(\text{sea})} - p\text{CO}_{2(\text{air})}) \quad (1)$$

where k is the gas transfer velocity, and $p\text{CO}_{2(\text{sea})}$ and $p\text{CO}_{2(\text{air})}$ represent the partial pressure of CO₂ in the surface ocean and atmosphere, respectively. The biological production term in the model is composed of

$$J_{\text{bio}} = -r(T, L) \cdot P \cdot \frac{N}{N + N_o} + P(\text{CaCO}_3) + g \cdot Z \cdot \varepsilon_{\text{her}} \cdot (1 - \text{zinges}) \cdot \frac{(P - P_{\text{min}})}{P + P_o} + d_o \cdot \frac{N}{N + k_{\text{doc}}} \cdot \text{DOC} + l_o \cdot \text{POC} \quad (2)$$

$$r(T, L) = \pi \cdot \frac{f(T) \cdot f(L)}{\sqrt{f(T)^2 + f(L)^2}} \cdot \frac{\text{Fe}}{(\text{Fe} + k_{\text{Fe}})} \quad (3)$$

$$P(\text{CaCO}_3) = A(P_{\text{orgC}} - 0.5 \cdot P_{\text{BSi}}) \quad (4)$$

$$f(T) = a \cdot b^{cT} \quad (5)$$

$$f(L) = L \cdot \beta \cdot \text{PAR} \quad (6)$$

All parameters in Eqs. (2) to (6) are described in Table 1. The terms in Eq. (2) represent primary production (r), calcium carbonate production ($P(\text{CaCO}_3)$), and remineralization of the following: non-assimilated zooplankton (Z) grazing, dissolved organic carbon (DOC), and particulate organic carbon (POC). Primary production depends on regionally varying growth rates and nutrient concentration $N = \min(\text{PO}_4, \text{NO}_3 \cdot R_{P:N})$, where $R_{P:N}$ represents the phosphate-to-nitrate Redfield ratio. The growth rate of phytoplankton (P) is a function of light (L), temperature (T), and dissolved iron (Fe), as shown in Eq. (3). Calcium carbonate production is a function of organic and silicate production in the euphotic layer. In this model, the phytoplankton compartment consists of two functional groups, diatoms and calcifiers. The concentration of both diatoms and calcifiers are determined

Table 1. Description of ecosystem parameters.

Symbol	Description	Values/Unit
<i>A</i>	Calcium carbonate production parameter	0.2
DOC	Dissolved Organic Carbon	[$\mu\text{mol C/L}$]
Fe	Dissolved iron	[nmol Fe/L]
<i>L</i>	Light (Incoming shortwave radiation)	[W m ⁻²]
<i>N</i>	Nutrient	[$\mu\text{mol C/L}$]
<i>N_o</i>	Nutrient half saturation constant	0.016 [$\mu\text{mol P/L}$]
<i>P</i>	Phytoplankton	[$\mu\text{mol C/L}$]
<i>P_{min}</i>	Minimum concentration of phytoplankton	0.01 [$\mu\text{mol C/L}$]
<i>P_o</i>	Phytoplankton half saturation constant	4 [$\mu\text{mol C/L}$]
<i>P_{orgC}</i>	Organic carbon production	[C m ⁻² day ⁻¹]
<i>P_{BSi}</i>	Biogenic silica parameter	[Si m ⁻² day ⁻¹]
PAR	Photosynthetically active radiation	0.4
POC	Particulate Organic Carbon	[$\mu\text{mol C/L}$]
Si	Silicate	1.0 [$\mu\text{mol C/L}$]
<i>T</i>	Temperature	[°C]
<i>Z</i>	Zooplankton	[$\mu\text{mol C/L}$]
<i>a</i>	Maximum phytoplankton growth parameter	0.81 [day ⁻¹]
<i>b</i>	Growth rate at 0°C	1.066
<i>c</i>	Temperature dependence of phytoplankton growth	1.0
<i>d_o</i>	Remineralization rate of DOC	0.005 [day ⁻¹]
<i>g</i>	Zooplankton grazing rate	0.5 [day ⁻¹]
<i>k_{doc}</i>	Half-saturation constant for DOC	0.5 [$\mu\text{mol P/L}$]
<i>k_{Fe}</i>	Iron half saturation constant	0.01 [nmol Fe/L]
<i>K_{Si}</i>	Silicate half saturation constant	0.01 [$\mu\text{mol C/L}$]
<i>l_o</i>	POC remineralization rate	0.0033 [day ⁻¹]
<i>zings</i>	Zooplankton assimilation efficiency	0.5 [day ⁻¹]
β	Initial slope of P-I curve	0.005 [m ² (W day) ⁻¹]
ϵ_{her}	Herbivores ingestion parameter	0.8
π	Phytoplankton growth rate parameter	1.0 [day ⁻¹]

as a function of simulated phytoplankton and silicate concentration.

$$\frac{\partial \text{diatoms}}{\partial t} = \frac{\partial P}{\partial t} \cdot \frac{Si}{(Si + k_{Si})} \quad (7)$$

$$\frac{\partial \text{calcifiers}}{\partial t} = \frac{\partial P}{\partial t} \cdot \left[1 - \frac{Si}{(Si + k_{Si})} \right] \quad (8)$$

The model simulates the main characteristics of ocean biogeochemistry, such as the distribution of the major biochemical tracers, including phosphate, nitrate, iron, dissolved inorganic carbon, alkalinity, and radiocarbon. In addition, it resolves some of the High Nutrient-Low Chlorophyll (HNLC) regions in the world by implementing iron-limited productivity. Compared to a more computationally expensive, high-resolution ocean model, this model allows us to efficiently apply the adjoint technique in order to study the large-scale pattern of the biogeochemical state throughout the water column. Due to the relatively short, 10-year integration of the simulations, the sediment module is simplified by introducing a sink-only sediment layer (see Tjiputra, 2007).

For the experiment with the anthropogenic CO₂ forcing, the model is first integrated from year 1825 to 1995, offline, with seasonally varying climatological fields (advective flow fields, potential temperature, salinity, surface air temperature, wind velocity, sea surface elevation, sea-ice distribution). The anthropogenic CO₂ forcing is taken from a spline fit to ice core and Mauna Loa CO₂ data (Enting et al., 1994; Wetzel et al., 2005). The adjoint sensitivity experiments are conducted from 1995 through 2005 based on similar forcings as above. In order to evaluate the simulated seasonal cycle and net annual sea-to-air CO₂ flux, we compared those fields to global observations from Takahashi et al. (2002) (<http://www.ldeo.columbia.edu/res/pi/CO2/>), averaged both monthly and annually, and interpolated onto the model grid. The simulated seasonal cycle of the sea-to-air CO₂ flux in different ocean locations (e.g. Bermuda Atlantic Time-Series Study (BATS), Hawaii Ocean Time-Series (HOTS) and Southern Ocean, 56° S, 275° W) generally follows the observations (Fig. 1), but there is a 2-month phase lag in the Southern Ocean that may be attributed to

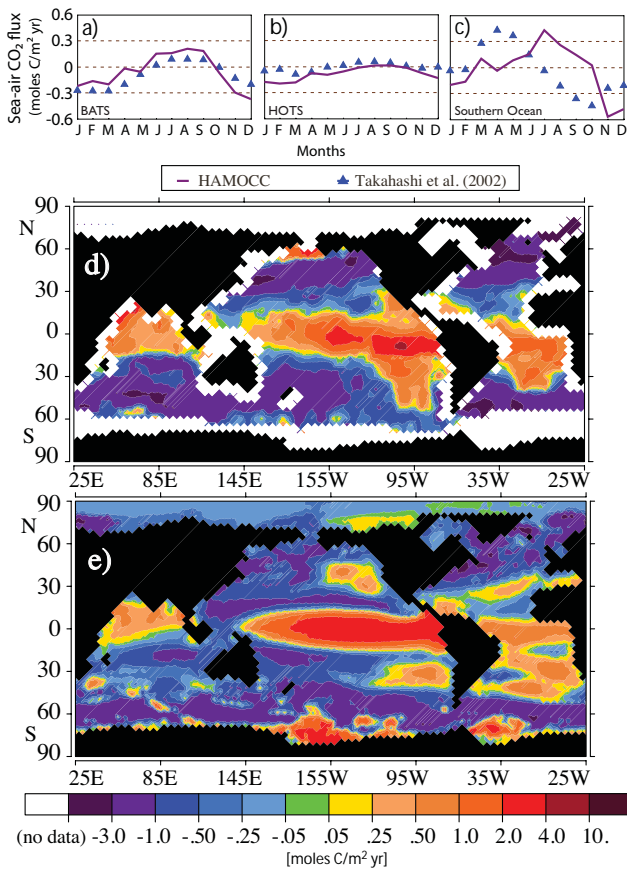


Fig. 1. Simulated seasonal cycle of sea-to-air CO₂ flux (moles CO₂ m⁻²yr⁻¹) at (a) Bermuda Atlantic Time-Series Study (BATS), (b) Hawaii Ocean Time-Series (HOTS), and (c) Southern Ocean (56° S, 275° W) with observational estimates from Takahashi et al. (2002). Averaged sea-to-air CO₂ flux for the year 1995 estimated from (d) observations by Takahashi et al. (2002) and (e) from HAMOCC5 model simulation. Positive values represent outgassing to atmosphere, whereas negative values indicate uptake of CO₂ from the atmosphere. The observations reveal local variability, which is not reproduced by the model, perhaps owing to grid-resolution or approximations in the equations of motions.

the location and timing of convective mixing in the model as well as the parameterization of the biogeochemistry in this region. Sparse pCO₂ and wind-speed data in the Southern Ocean also lead to substantial uncertainties in the gridded data-based product of the sea-air CO₂ flux in that region (Takahashi et al., 2002; Gloor et al., 2003). In addition, high wind speeds observed in the Southern Ocean increase the uncertainty in the CO₂ gas transfer rate (Sabine et al., 2004). Figure 1 shows that the annual average sea-to-air CO₂ flux map for 1995 simulated by the model follows the general observed patterns, including outgassing in the equatorial oceans due to upwelling of colder, CO₂-rich subsurface waters and carbon uptake that is prominent in the subtropical western boundary and high latitude convective mixing regions. Yet

in the subpolar North Pacific, namely the Bering Sea, the model does not simulate the strong outgassing that is observed. That artefact may be due to the low model resolution and shortcomings in the model seasonal mixed-layer depth parameterization.

2.2 Adjoint sensitivity

Takahashi et al. (2002) analyzed the seasonal variability of surface pCO₂ due to different components and discussed their relative significance in different regions based on their gridded climatological data-based product. However, they differentiated only between thermal- and nonthermal-driven variability, often referring to the latter as biological activity. In contrast, we use an intermediate complexity, adjoint, carbon-cycle model to analyze the variability due to all thermal and nonthermal components (Sect. 3.1).

In the model, the total seasonal change of the partial pressure of CO₂ in the surface ocean depends on its DIC concentration, sea surface temperature (SST), alkalinity (TALK), and the salinity (S) (Le Quéré et al., 2000; Wetzel et al., 2005)

$$\frac{dpCO_2}{dt} \approx \frac{\partial pCO_2}{\partial DIC} \frac{dDIC}{dt} + \frac{\partial pCO_2}{\partial T} \frac{dT}{dt} + \frac{\partial pCO_2}{\partial TALK} \frac{dTALK}{dt} + \frac{\partial pCO_2}{\partial S} \frac{dS}{dt} \quad (9)$$

Here, the seasonal cycle of surface pCO₂ due to each component in Eq. (9) is calculated separately. The adjoint model is applied to calculate the monthly partial derivative terms (i.e., $\frac{\partial pCO_2}{\partial DIC}$, $\frac{\partial pCO_2}{\partial T}$, $\frac{\partial pCO_2}{\partial TALK}$, $\frac{\partial pCO_2}{\partial S}$). Additionally, the DIC component is further decomposed into different biophysical components. The contribution from each component is discussed in Sect. 3.2.

The adjoint model also provides an efficient means to estimate the sensitivity of the simulated sea-to-air CO₂ flux to small perturbations in model input or control parameters. This adjoint sensitivity analysis is equivalent to thousands of forward perturbation runs, but it is made at only a fraction of the computational expense by running one forward and one adjoint model integration. Here, the adjoint codes have been generated by the TAMC (Tangent linear and Adjoint Model Compiler) (Giering and Kaminski, 1998; www.fastopt.com) and improved manually to be more computationally efficient. The accuracy of the adjoint code has been tested using a finite-difference approximation. The cost function is defined as the global, area-integrated, sea-to-air CO₂ flux (F_{CO_2}) over 1995–2005 denoted as

$$J_{FCO_2} = \iint F_{CO_2} dAdt \quad (10)$$

where A represents the area of the specific model grid and t represents time integration. The sensitivity map in this study is produced by applying the adjoint model to estimate the partial derivative of the cost function to a small perturbation

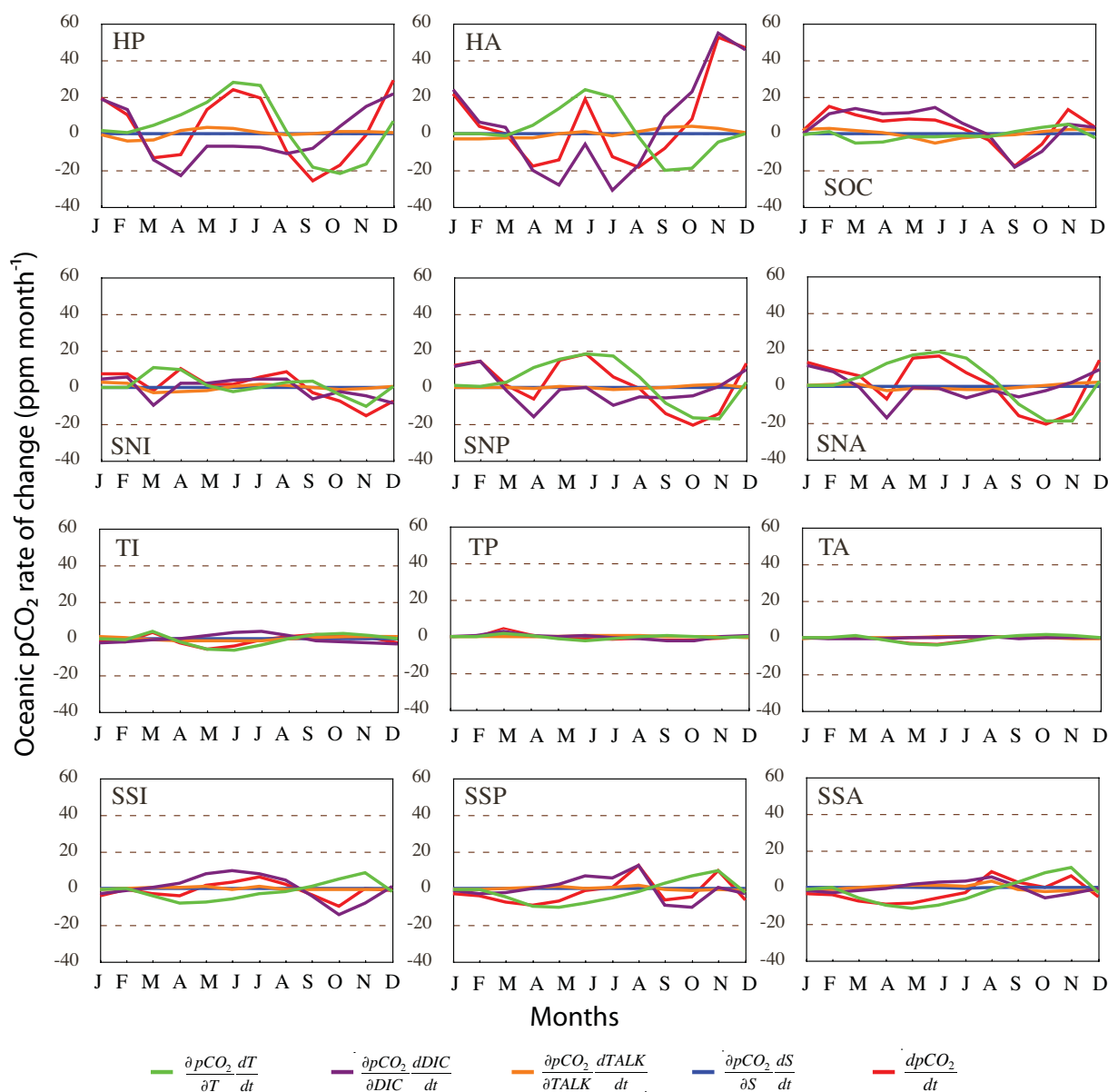


Fig. 2. Seasonal cycle of the total change in oceanic pCO₂ and corresponding contributions (Eq. 9) from changes in SST, DIC, alkalinity, and salinity for different ocean regions. Ocean regions are defined as follows: high latitude Pacific (HP, north of 50° N), high latitude Atlantic (HA, north of 50° N), Southern Ocean (SOC, south of 50° S), subtropical (14° N–50° N) North Indian (SNI), subtropical North Pacific (SNP), subtropical North Atlantic (SNA), tropical (14° N–14° S) Indian (TI), tropical Pacific (TP), tropical Atlantic (TA), subtropical (14° S–50° S) South Indian (SSI), subtropical South Pacific (SSP), and subtropical South Atlantic (SSA). Units are in ppm month⁻¹.

of a specific control variable α , such that the sensitivity at each model grid cell is represented by $\partial J_{\text{FCO}_2} / \partial \alpha_{(x,y)}$.

To investigate nutrient contributions to the sea-to-air CO₂ flux, the adjoint model is applied to estimate the regional sensitivity to perturbations of nutrient concentration $\partial J_{\text{FCO}_2} / \partial N_{(x,y)}$. Both the forward and the adjoint models are integrated for ten years with a monthly input of surface nitrate (0.008 mol N/m²), phosphate (0.0005 mol P/m²), and iron (1.65 $\mu\text{mol Fe/m}^2$) concentrations in three separate ex-

periments. The perturbation is adjusted toward the Redfield ratio (N:P:Fe=16:1:3.3 $\times 10^{-3}$, for example, a perturbation of 0.008 mol nitrate is assumed to be comparable with a perturbation of 0.0005 mol phosphate). This adjustment is crucial since a perturbation of a different magnitude could result in different sensitivities.

Table 2. Monthly correlation coefficient R computed over annual (one-year) and seasonal periods in 1995 between pCO₂ and SST and between pCO₂ and DIC.

	Annual		JFM		AMJ		JAS		OND	
	SST	DIC	SST	DIC	SST	DIC	SST	DIC	SST	DIC
HA	-0.110	0.898	0.670	0.999	0.916	0.899	-0.387	0.592	0.934	0.990
HP	0.667	0.496	-0.887	0.992	0.935	0.953	0.995	0.404	0.983	0.960
SNA	0.766	0.440	-0.813	0.967	0.967	0.997	0.987	0.046	0.989	0.964
SNI	0.535	0.745	-0.999	0.999	0.952	-0.341	-0.453	0.974	0.891	-0.157
SNP	0.741	0.525	-0.993	0.999	0.966	0.997	0.987	-0.633	0.983	0.977
TP	0.711	0.863	0.991	0.992	0.936	0.568	0.328	0.021	0.106	0.933
TA	0.974	-0.299	0.933	-0.344	0.999	-0.942	0.935	-0.497	0.973	-0.489
TI	0.876	-0.255	0.999	0.972	0.876	-0.461	0.999	-0.991	0.999	0.948
SSP	0.412	0.607	0.952	0.325	0.905	0.999	-0.439	0.938	0.740	0.688
SSA	0.745	0.114	0.983	-0.107	0.438	0.888	0.575	0.459	0.939	-0.565
SSI	-0.351	0.805	0.403	0.360	0.784	0.999	-0.997	0.989	-0.127	0.744
SOC	-0.124	0.900	0.055	0.871	0.812	0.010	-0.837	0.999	0.274	0.908

3 Results

3.1 Seasonal variability of pCO₂

Figure 2 shows the seasonal cycle of surface pCO₂ due to the variability of DIC, SST, alkalinity, and salinity in different ocean regions following the approach of Takahashi et al. (2002). The variability of the sum of all components has been confirmed using the differential of monthly output of the forward model. In general, the total change of pCO₂ in Eq. (9) is mainly influenced by the temperature and DIC terms. In the tropical regions (14° N–14° S), the seasonal variability is relatively small, with the exception of the Indian Ocean, perhaps owing to the Indian Ocean Monsoon. In the tropical Atlantic and Indian Oceans, the annual cycle of pCO₂ is mostly controlled by SST variability, whereas both DIC and SST variability control pCO₂ annual cycle in the tropical Pacific. In the subtropical Pacific and Atlantic, where warm tropical water meets colder water from higher latitudes, the temperature terms are more important than the DIC term. For example, during summer time, the warm SST promotes high surface pCO₂, which is affected by strong stratification and lower solubility of warm water. In the fall and early winter, rapid cooling of SST increases CO₂ solubility and reduces surface pCO₂.

In the higher latitudes of the North Atlantic (north of 14° N) and Southern Ocean, the annual cycle of pCO₂ is largely controlled by the DIC term. The large variability of DIC in these regions is due to the strong wintertime convective mixing and rapid springtime biological drawdown. In the subarctic Pacific, where the model potentially underestimates DIC variability, perhaps due to unresolved mixing processes near the Bering Strait, the SST variability dominates. During boreal summer months (July to September), the SST

component dampens the DIC-driven pCO₂ variability in all northern high-latitude regions.

Table 2 summarizes one-year and seasonal correlation coefficients between pCO₂ and SST as well as between pCO₂ and DIC. The correlation coefficient is computed based on spatial, within specified regions, monthly correlation computed over one year and each seasonal period. The inner annual variability of surface pCO₂ observed at the Bermuda Atlantic Time-series Study (BATS) station is mainly regulated by temperature variability (e.g. Takahashi et al., 2002). Similarly, the spatial correlation coefficient R , over one-year period, between pCO₂ and SST in the subtropical North Atlantic region estimated by this study is $R=0.766$, compared to only $R=0.440$ for the correlation with DIC. More detailed analysis shows that the warming of surface SST increases surface pCO₂ as early as February and lasts until the beginning of August, when there is a general cooling over the rest of the year. In contrast, DIC variability controls surface pCO₂ only by photosynthetic activity during spring (March to May) and by upwelling of DIC-rich subsurface water in the winter (November to January) periods (see also Fig. 3, NA).

The observed annual cycle of pCO₂ at Weather Station P in the North Pacific indicates that DIC variability reduces surface pCO₂ during both the early spring and summer. Furthermore, the observed uptake during the early spring is much weaker than the summer time (Takahashi et al., 2002). Here, the simulated reduction of springtime pCO₂ due to DIC in the high latitude Pacific (HP in Fig. 2) is greater than that estimated by Takahashi et al. (2002). One explanation for this discrepancy is that we consider a larger area, the entire subarctic Pacific region, which also encompasses the western subarctic gyre known for its stronger convective mixing

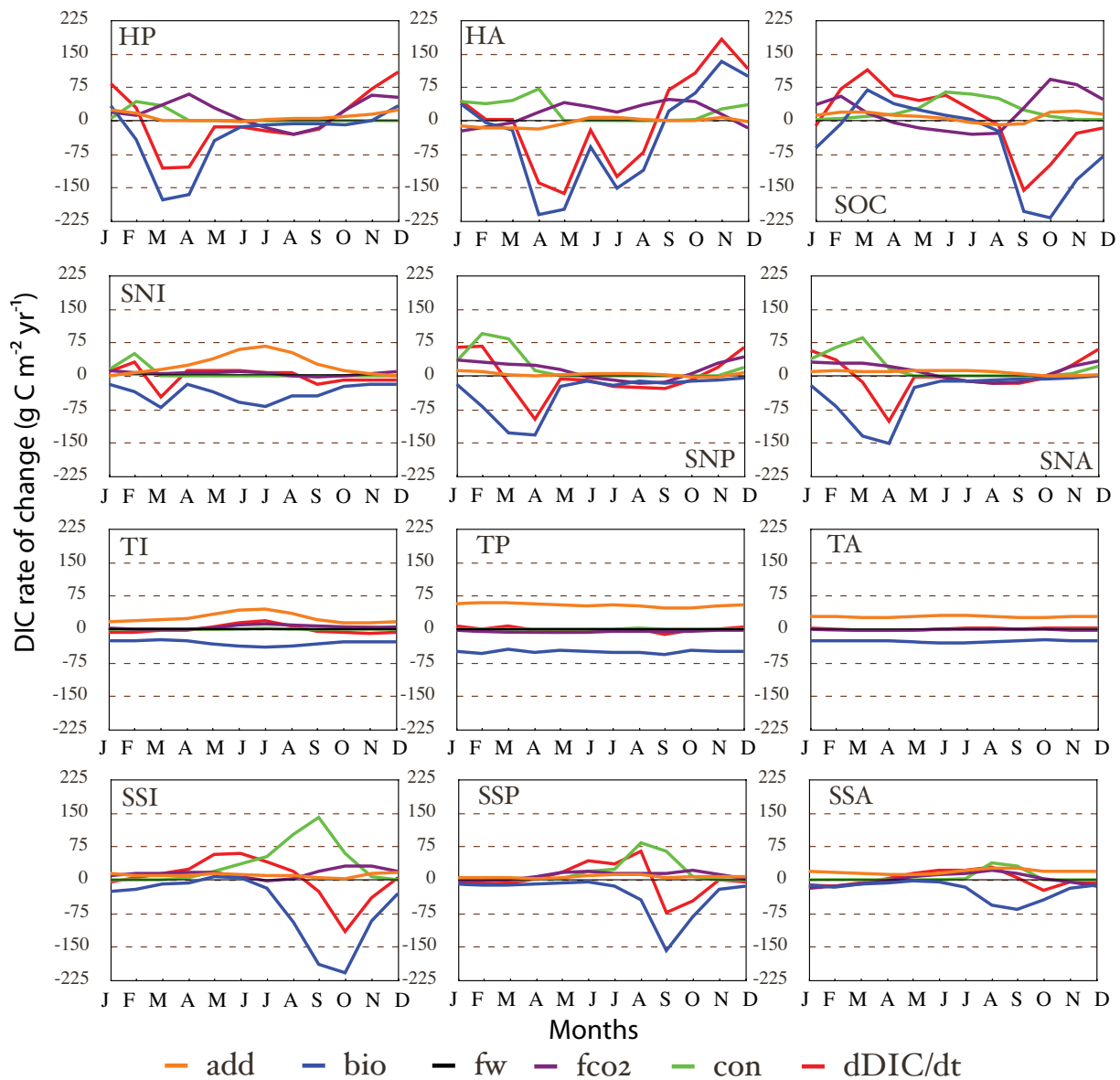


Fig. 3. Seasonal cycle of the total change of dissolved inorganic carbon (DIC) and the contributions to the total change (Eq. 11) from advection, biology, fresh water flux, sea-to-air CO₂ flux, and convective mixing. Ocean regions are the same as in Fig. 2. Units are in g C m⁻²yr⁻¹.

and seasonal variability (Chierici, et al., 2006). Such strong physical variability is generally not observed at Weather Station P. The reduction of surface pCO₂ during spring is mainly due to biological processes, which exploit high-nutrient concentration supplied by convective mixing. For instance, observed phosphorus in the western subarctic Pacific indicates strong uptake begins as early as April (Conkright et al., 2002; McKinley et al., 2006). In summer, stratification due to SST warming reduced DIC uptake by biological activity. The spatial seasonal correlation coefficients in Table 2 indicate that the variability of pCO₂ in the subarctic Pacific (NP) is mostly dominated by the DIC in the spring months and by SST in the summer months.

In the tropical Pacific, Table 2 shows that surface pCO₂ variability is highly correlated with SST during the boreal spring ($R=0.936$) whereas DIC variability mostly dominates in the fall ($R=0.933$). This result is also consistent with the study by Feely et al. (2006), which observes lower seawater CO₂ fugacity in the boreal fall than in the spring in the equatorial Pacific. This difference is associated with fall upwelling of carbon- and nutrient-rich water, which increases biological productivity. In contrast, strong warming of SST in spring increases surface pCO₂ (Wang et al., 2006).

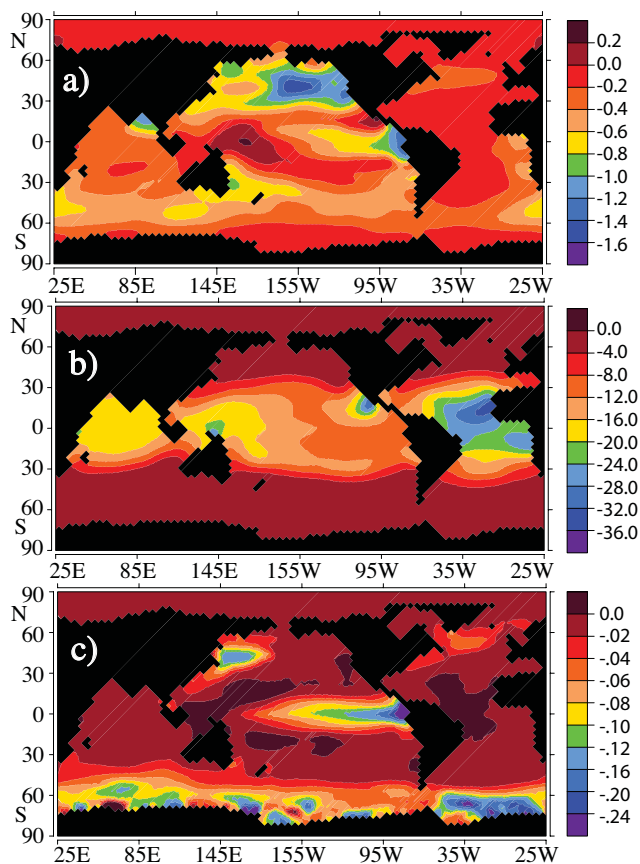


Fig. 4. Regional sensitivity of the accumulated global sea-to-air CO₂ flux over a ten-year period (see Eq. 10) in terms of monthly perturbation of (a) nitrate units in Pg C/(mol N m⁻²), (b) phosphate Pg C/(mol P m⁻²), and (c) iron Pg C/(mmol Fe m⁻²). Negative values indicate that an increase in the nutrient will increase the uptake of CO₂ from the atmosphere. Positive values indicate the opposite.

3.2 Seasonal variability of DIC

We further decomposed seasonal variability of surface DIC into different biophysical components. The change in simulated DIC is separated into sources and sinks from transport (advection and diffusion), biological activity, fresh water fluxes, sea-to-air CO₂ exchange, and convective mixing:

$$\frac{dDIC}{dt} \approx J_{add} + J_{bio} + J_{fw} + J_{FCO_2} + J_{con} \quad (11)$$

Figure 3 shows the annual cycle of each component in Eq. (11) for different ocean regions. In general, the fresh water flux and the sea-to-air CO₂ flux components have only minor contributions to the overall DIC variability. In almost all regions, the biology term has stronger seasonal amplitude than the other terms. The biological productivity during spring and summer periods reduces the surface DIC concentration. During winter periods in both hemispheres, the strong convective mixing contributes to the strong outgassing of ocean CO₂, whereas during summer the surface layers are

more stratified. In the tropical regions, the advection term, which is dominated by continuous upwelling, has the same magnitude as the biological term, but both terms cancel one another nearly entirely. The equatorial Pacific region has the highest accumulated, biologically driven, net carbon loss (approximately 50 g C m⁻² yr⁻¹). In the mid latitudes, DIC variability is dominated by biological and convective mixing terms. But the relative strength of biological activity is opposite in sign and is roughly twice as large as the convective mixing term. At the end of spring in each hemisphere, the contribution from convective mixing drops to zero, as summer stratification sets in.

In the higher latitudes, DIC variability is generally dominated by biological activity. In late winter of both hemispheres, strong convective mixing brings up subsurface DIC and nutrients that increase surface DIC, followed immediately by strong uptake of DIC by biological production. For example, in the high-latitude North Atlantic (see Fig. 3, HA), the model has strong convective mixing from November to April. This strong mixing results in deepening of the mixed layer and increases DIC and nutrient fluxes from subsurface waters. Consequently, the biological production starts to drawdown DIC in the early spring. Later in the summer, after nutrients are exhausted, there is strong reduction in biological uptake. In situ observations by Olsen et al. (2007) indicate similar characteristics for the convective mixing and spring bloom, but they also indicate that biologically driven uptake of surface DIC persists through summer, unlike in the model. This discrepancy may indicate that the model remineralizes organic matter too slowly in this location. In addition, the model does not explicitly include flagellates, which may also contribute to the misfit. In the North Atlantic, flagellates are known to be an important short-lived phytoplankton component during summer, which help transfer carbon to higher trophic levels via DIC uptake (Richardson et al., 2000; Schrum et al., in press). The ocean pCO₂ observations also indicate that the sea-air CO₂ flux is substantial only during summer and fall when the water is more stratified, which is consistent with the model. The model's average biologically driven carbon uptake in the North Atlantic is 34 g C m⁻² yr⁻¹.

Simulated variability in the high-latitude North Pacific and Southern Ocean are comparable to changes in the high-latitude North Atlantic. In the subarctic North Pacific, the average net carbon loss due to biological activity is 34 g C m⁻² yr⁻¹. However, observations have indicated that biological uptake in this region varies greatly from 23 to 64 g C m⁻² yr⁻¹ due to high physical variability between the western and eastern gyres (Chierici et al., 2006). Relatively stronger uptake by biological activity is simulated in the Southern Ocean, 49 g C m⁻² yr⁻¹. Overall, the biological uptake of DIC per m² is largest in the Southern Ocean, subtropical south Indian Ocean, and high-latitude North Atlantic Ocean. Maximum uptake reaches nearly 225 g C m⁻² yr⁻¹ in the spring period of each hemisphere.

3.3 Sensitivity of sea-to-air CO₂ flux to nutrients

The sensitivities of the sea-to-air CO₂ flux to perturbations of nitrate, phosphate, and iron are shown in Fig. 4. The global sea-to-air CO₂ flux is highly sensitive to nitrate perturbations in the northeast Indian, the northeast Pacific, and the eastern equatorial Pacific Oceans. There is moderate sensitivity in the Southern Ocean and low sensitivity for the other regions. Ocean carbon uptake is most sensitive toward phosphate addition in the equatorial and subtropical regions. The highest sensitivities are found just off the coast of northwest Africa followed by the west coast of Mexico, the western equatorial Pacific Ocean, and the Indian Ocean. The sensitivity map shows that monthly addition of one mol of phosphate per m² over a model grid in the coast for northwest Africa (i.e., 10°–20° N, 2.5×10⁵ km²) over a period of ten years would result in approximately 36 Pg of atmospheric carbon uptake (i.e., 1.5×10³ ton C/ton PO₄ month⁻¹). To put this into context, this phosphate addition would require approximately 3.6 times the total world production of phosphorus fertilizer in 2007 (0.387 Pg P₂O₅, FAO, 2008). The sensitivity maps show that the carbon uptakes have low sensitivity toward phosphate in the high latitude.

The sensitivity of the sea-to-air CO₂ flux toward regional iron fertilization indicates a remarkable response in the eastern equatorial Pacific, western North Pacific, and the Southern Ocean. There is generally low sensitivity throughout the other ocean regions. These iron sensitivity results generally compliment previous studies (de Baar et al., 1995; Gnanadesikan et al., 2003; Zeebe and Archer, 2005; Aumont and Bopp, 2006; Parekh et al., 2006). In a model grid in the eastern equatorial Pacific (i.e. 3×10⁵ km²), the sensitivity results indicated an uptake of approximately 0.24 Pg C could result from monthly fertilization of one mmol Fe per m² within ten years period (approximately 1.4×10⁴ ton C/ton Fe month⁻¹). In the Southern Ocean, the patchy sensitivity regions are due to regional differences in timing and strength of convective mixing. A recent study by Dutkiewicz et al. (2006) applied similar approach in determining the sensitivity of global sea-to-air flux to bioavailable iron with a simplified carbon cycle model without ecosystem dynamics. Our study generally reproduced the regional sensitivity of their study. However, Dutkiewicz et al. (2006) find a stronger sensitivity of the global sea-to-air CO₂ flux to iron in the equatorial Pacific, probably because of their lower simulated iron concentration in the equatorial Pacific Ocean. The lower iron concentration in their model may also be related to their iron input function, which account only for dust deposition, but not the sedimentary source (Aumont and Bopp, 2006). Observations of dissolved iron are sparsely distributed, making the model validation difficult (Parekh et al., 2005). In addition, in the northeast subarctic Pacific Ocean, our adjoint model shows little sensitivity of carbon uptake to iron fertilization, whereas observation indicates otherwise (e.g. Boyd et al., 1998). This discrepancy may be due to the unrealistic

simulated circulation, which is a common problem in most coarse-resolution model (McKinley et al., 2006).

3.4 Sensitivity of sea-to-air CO₂ flux to ecosystem parameters

To assess how modelled plankton activity affects simulated sea-to-air CO₂ exchange, its regional sensitivity to ecosystem parameters are estimated using the adjoint model. Earlier regional and global adjoint sensitivity studies (e.g. Zhao et al., 2005; Tjiputra et al., 2007) indicated that maximum phytoplankton growth, phytoplankton exudation, zooplankton grazing, and zooplankton excretion are all sensitive ecosystem parameters. Thus we analyzed the sensitivity of the sea-to-air CO₂ flux to these control variables. All the control parameters are normalized to be ratios between the a posteriori and the a priori control parameters (i.e. $\alpha_n = (\alpha_n^{\text{aposteriori}} / \alpha_n^{\text{apriori}})$, Giering, 1989). The adjoint model is applied to calculate $\partial J_{\text{FCO}_2} / \partial \alpha_{n(i,j)}$, where n represents the parameter type domain. Generally, the global sea-to-air CO₂ flux is sensitive to these ecosystem parameters in regions having large annual productivity, including the equatorial Pacific, the North Pacific western gyre, the North Atlantic, and the Southern Ocean.

For the phytoplankton growth rate parameter (π in Eq. 3), the carbon uptake is most sensitive in the equatorial Pacific, North Pacific, and North Atlantic (Fig. 5a). Continuous upwelling and strong convective mixing in these regions supply the essential nutrients to fuel phytoplankton growth. Therefore, increasing growth rate increases photosynthesis, which reduces the surface DIC concentration. In the subtropical Pacific and subtropical Atlantic regions, there are positive sensitivities of the sea-to-air CO₂ flux to increases in phytoplankton growth rate. In these oligotrophic regions, a higher phytoplankton growth rate will initially increase the productivity and uptake of atmospheric carbon, but over longer periods (5 years), the phosphate will be depleted because there would be less supply of new nutrients from below the euphotic zone. Subsequently, this condition leads to reduction in the overall biological productivity, and hence an increase in ocean outgassing.

The exudation rate parameter controls the dissolved organic carbon released by phytoplankton respiration. In most regions with a continuous supply of nutrients from below the euphotic zone, the increase in the exudation rate leads to reduction in the phytoplankton concentration and biological production rate, both of which would increase the surface pCO₂ and ocean CO₂ outgassing. However, in the oligotrophic regions (e.g., the subtropical North Pacific and subtropical South Pacific), an increase in exudation rate increases the dissolved organic carbon (DOC) concentration at the surface. Therefore, over longer time scales, it will enhance regenerated nutrients, which increases photosynthesis and carbon uptake. Figure 5b shows that over the ten-year period, increasing phytoplankton exudation rate increases

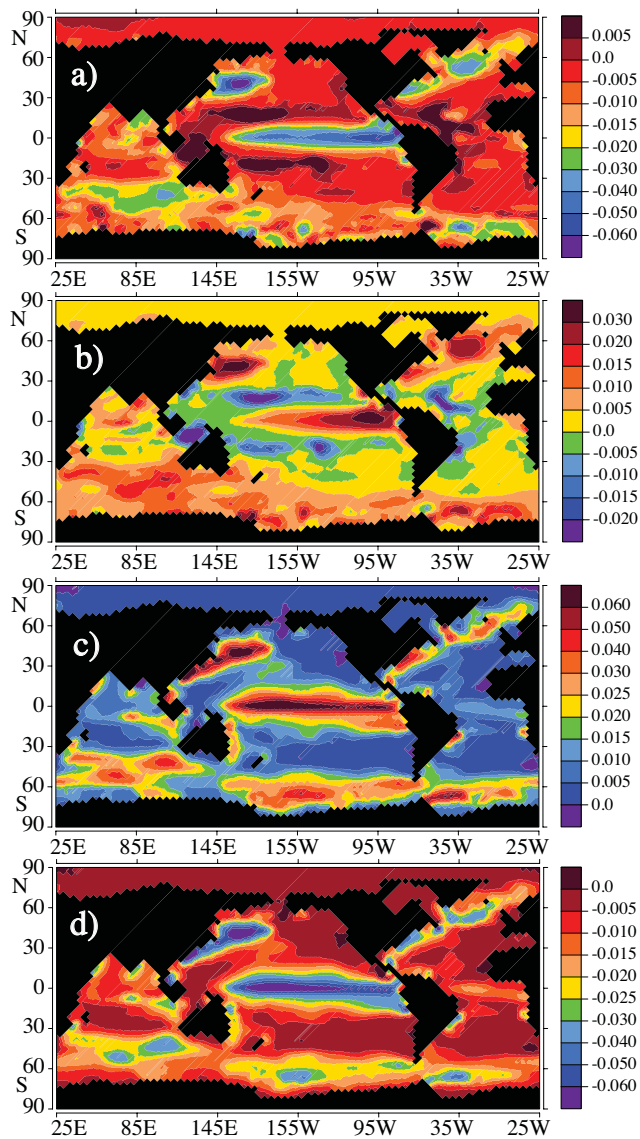


Fig. 5. Regional sensitivity map of the global sea-to-air CO₂ flux in terms of (a) phytoplankton maximum growth rate, (b) phytoplankton exudation, (c) zooplankton grazing, and (d) zooplankton excretion parameters integrated over ten years period. Negative values indicate that an increase in the parameter will increase uptake of CO₂ from the atmosphere. Units are in Pg C.

carbon uptake in the subtropical, oligotrophic regions, but decreases carbon uptake in the equatorial Pacific, Northwest Pacific, North Atlantic, and the Southern Ocean.

Both in the ocean and lake ecosystems, zooplankton play an important role in controlling nutrient uptake (i.e. primary production) by phytoplankton (Moore et al., 2002; Pasquer et al., 2005; Schindler et al., 1997; Smetacek, 2001). For example, in situ observations have shown that lakes with low zooplankton biomass tend to take up atmospheric CO₂, whereas lakes with high zooplankton biomass tend to do the oppo-

site (Carpenter et al., 2001). In this study, we show that in regions where the sea-to-air CO₂ flux is controlled by the biological component, the surface carbon fluxes are sensitive to the grazing parameter g (Eq. 2). Figure 5c illustrates that in regions with strong upwelling and convective mixing, reducing the grazing rate would substantially increase the uptake of atmospheric CO₂. The results agree with previous sensitivity studies with one-dimensional forward models (Chai et al., 2002; Dugdale et al., 2002), which indicated that in the equatorial Pacific the sea-to-air CO₂ flux and surface pCO₂ are sensitive to grazing parameters. Furthermore, the simulated sea-to-air CO₂ fluxes in the North Pacific and Southern Ocean also respond to variations in the grazing parameter. In these regions, reduced grazing increases phytoplankton biomass in the euphotic zone, thus increasing nutrient and DIC uptake by photosynthesis. Figure 5c also shows strong sensitivity toward the grazing parameter at the Bermuda Atlantic Time-series Study (BATS) site, because the grazer community consumes most of the production at this location, which is consistent with in situ measurements from Lessard and Murrell (1998).

Figure 5d shows that the regional sensitivity of carbon uptake to zooplankton excretion parameters is nearly identical to that for grazing parameters, but with opposite signs. The excretion rate parameter mainly controls the dissolved organic carbon released by zooplankton. Hence, it controls the balance between new and regenerated nutrients, which affect the biogeochemical cycle and carbon sequestration in the ecosystem. Contrary to the grazing rate parameter, a reduction in the excretion rate increases the zooplankton mass and hence increases the zooplankton grazing pressure. Consequently, the rate of photosynthesis and DIC uptake would be reduced. In addition, the concentration of DOC is reduced when the excretion rate is small, reducing the amount of organic matter that is immediately recycled into nutrients in the euphotic zone. In the oligotrophic subtropical regions, Popova et al. (2006) demonstrated that the zooplankton excretion rate regulates primary production by supplying regenerated nutrients, especially when zooplankton concentration is high. However, the adjoint model indicates that the global carbon uptake has little or no sensitivity to excretion parameters in this region, perhaps due to the relatively low regional zooplankton biomass throughout the year simulated by the model.

4 Discussion

Many studies (e.g. Maier-Reimer et al., 1996; Sarmiento et al., 1998; Cox et al., 2000; Fung et al., 2005; Le Quéré et al., 2005; Winguth et al., 2005; Friedlingstein et al., 2006; Hood et al., 2006) have indicated that future climate change would influence the marine biological pump and ecosystem dynamics. However, the current understanding on how the marine biological community would respond and

feedback on climate change is poorly constrained. Denman and Pena (2002) estimated an increase in planktonic physiological rates (e.g. phytoplankton growth, zooplankton grazing, and mortality rate) due to warming. However, the magnitude, extent, and duration of these consequences remain open questions and changes would likely vary regionally. For example, Wrona et al. (2006) projected that, in the Arctic region, permafrost thawing would increase the marine nutrient and carbon delivery to the ocean and could alter the transformation and partitioning of carbon by marine ecosystem within this region. In high-latitude regions, Bopp et al. (2001) demonstrated that phytoplankton growing season and export production increase in response to future climate change. To further assess how these processes may affect the feedback processes in the global carbon cycle, it is valuable to understand how the sea-to-air carbon flux would respond to changes in marine plankton dynamics.

In the subtropical North Atlantic gyre, the sensitivity analysis of sea-to-air CO₂ fluxes to changes in phosphate and nitrate concentration shows that the carbon uptake is more sensitive to perturbations of phosphate than those of nitrate. This greater response to changes in simulated phosphate can be linked to a phosphate-depleted environment, which is induced by high phytoplankton growth stimulated by nitrogen fixation (i.e. by cyanobacteria). In contrast, marine ecosystem models without nitrogen fixers indicate that the global ocean is most likely to be nitrogen-limited with N:P < 16 (Moore et al., 2004). Nitrogen fixation is particularly important to maintain biological productivity when the N:P ratio becomes too low (Tyrell, 1999). Most of the nitrogen fixation by cyanobacteria simulated by the model occurs in warm (tropics and subtropics), and nitrate-depleted regions, such as the Indian Ocean, subtropical North Pacific, subtropical North Atlantic, and subtropical South Pacific. These features are consistent with observations and other model studies (Karl et al., 1997; Hoffmann, 1999; Wu et al., 2000; Boyd and Doney, 2002; Moore et al., 2004). Thus substantial nitrogen fixation reduces phosphate concentration in the above regions, resulting in phosphate limitation (Figure 4b). The high sensitivity in the North Atlantic is also attributed to its high dust input of iron, which allows more efficient macronutrient uptake for phytoplankton growth (Berman-Frank et al., 2001).

The simulated regional sensitivity of atmospheric carbon uptake to changes in physiological rate indicates that there are substantial regional variations. Uptake of atmospheric CO₂ by biological activity is most sensitive to changes in the physiological rate in regions with a continuous supply of nutrients from upwelling and convective mixing. In the model, these regions include the equatorial Pacific, western North Pacific, North Atlantic, and the Southern Ocean. In the high latitudes, studies by Bopp et al. (2001), Denman and Pena (2002), and Le Quéré et al. (2005) simulated an increase in phytoplankton growth rate in the future due to increased light availability (from shoaling of the mixed

layer depth) and increased temperature. In these regions, our adjoint sensitivity experiments indicate that an increase in only the phytoplankton growth rate would increase the uptake of atmospheric CO₂, especially in the equatorial and northwestern Pacific Ocean. On the other hand, shoaling of the MLD would decrease upwelling of nutrients (Cox et al., 2000; Fung et al., 2005), which could compensate for this enhanced carbon uptake. Despite the strong upwelling and mixing in the Southern Ocean, the carbon uptake simulated by the model is not sensitive to the phytoplankton growth rate. This is likely due to the extremely low dissolved iron concentration (i.e. approximately 0.1 nmol L⁻¹) simulated by the model in this location. The phytoplankton growth formulation in the model also depends on the dissolved iron concentration as shown in Eq. (3). Therefore, low concentrations of dissolved iron yield a lower phytoplankton growth rate and thus lower biological carbon uptake than in other regions where iron is not limiting.

The sensitivity map of sea-to-air CO₂ flux to ecosystem parameters indicates that in the high-nutrient, low-chlorophyll (HNLC) regions, such as the equatorial Pacific, the subarctic North Pacific, and the Southern Ocean, carbon uptake is sensitive to zooplankton grazing and excretion parameters. The sensitivity of zooplankton grazing in these locations confirms earlier sensitivity studies with one-dimensional forward models (Chai et al., 2002; Dugdale et al., 2002) as well as observation in the equatorial Pacific Ocean (Landry et al., 2003; Price et al., 1994). In addition, our simulated sea-to-air CO₂ flux in the North Pacific and Southern Ocean also responds to variations in the grazing parameter, consistent with the available observations (Landry et al., 2002; Saito et al., 2005). In these regions, an increase in the grazing rate suppresses phytoplankton mass in the euphotic zone, thereby reducing nutrient and DIC uptake by photosynthesis. Druon and Le Fevre (1999) demonstrated that increasing the zooplankton excretion rate in a one-dimensional, coupled physical-biological model could enhance the primary productivity in the North Atlantic. Since the zooplankton excretion rate regulates the zooplankton biomass, it would also help control the grazing pressure, hence biological production, over a longer period. Moreover, the excretion parameter regulates the flux of DOC that can be recycled into nutrients in the euphotic zone. For example, study by Sarma et al. (2003) demonstrated that zooplankton excretion is central in sustaining the high surface organic carbon demand, which cannot be met from supplies through circulation in certain regions, such as the Arabian and Indian Sea. Our sensitivity simulations show that an increase in zooplankton excretion rate reduces zooplankton concentration (and therefore grazing pressure) and increases the flux of regenerated nutrients, both of which lead to increase in primary production and carbon uptake in the equatorial Pacific, northwest Pacific, North Atlantic, Indian, and the Southern Ocean.

Despite the effectiveness of using an adjoint model to estimate the regional sensitivity, the variability of the sensitivity results are model-specific. Thus similar experiments with different models may yield different solutions. For example, the adjoint sensitivity also depends on the initial values of most of the control parameters (e.g., parameters listed on Table 1) in the model, which generally varies from one model to another. These parameters are determined based on observations and laboratory studies (e.g. Eppley, 1972; Amon and Benner, 1994), which do not necessarily represent the global marine ecosystem. Optimization techniques, such as the 4-DVAR method can provide more insight on how to better constrain these parameters (Zhao et al., 2005; Tjiputra et al., 2007). Moreover, other studies, such as Bopp et al. (2001) and Doney et al. (2004) demonstrate that physical properties (e.g. surface forcing, convective mixing parameterization, vertical and horizontal resolutions) of biogeochemical models can greatly alter carbon cycle model predictions. Furthermore, the current model used here does not consider interannual variability in physical forcing. The parameterization of the physical processes as well as model resolution both still require improvement. Given the dependency of the results of sensitivity analysis to the forward model, it would be valuable to conduct a similar adjoint sensitivity study with different carbon cycle models having different ecosystem parameterizations and physical flow fields.

5 Conclusions

In this study, the spatial variability of surface pCO₂ due to changes in SST, DIC, alkalinity, and salinity were estimated using an intermediate complexity, adjoint, global-scale, ocean carbon cycle model. In addition, we studied the biophysical factors that control regional DIC variability. Whereas other studies have focused on interannual variability (Le Quéré et al., 2005; Wetzel et al., 2005), we have focused on the annual cycle. The formulation of surface pCO₂ and DIC variability in our model were decomposed into different physical and biological components. The variability of surface alkalinity and salinity at the surface has little influence on the overall variability of seawater pCO₂. In the equatorial regions, the SST variability is the main factor controlling the pCO₂ variability. In the subtropical regions, the seasonal variability of surface pCO₂ is also dominated by SST variation, especially during the summer and fall seasons. In the subpolar regions, it is the seasonal variability of surface DIC that regulates most of pCO₂ annual cycle. These results confirm previous observational (Takahashi et al., 2002; Watson and Orr, 2003), and modeling studies (McKinley et al., 2004; Pasquer et al., 2005; Wetzel et al., 2005), but they are derived from an independent adjoint modeling approach.

The decomposition of DIC variability simulated by the model has helped identify the biological and physical processes that are the dominant controls of surface DIC vari-

ability. In equatorial upwelling regions, primary production is fueled by a continuous supply of upwelled nutrients, which decreases DIC concentrations in the surface layer. However, this nutrient-upwelling effect is compensated by simultaneous upwelling of colder, DIC-rich water. In the subtropics, convective mixing during winter increases surface DIC. Later, during spring and summer, the strong uptake of CO₂ by biological activity controls most of the surface DIC variability. In the high latitudes, the seasonal amplitude of surface DIC concentration is mostly determined by biological activity. Our decomposition analysis confirms previous studies that the uptake of atmospheric CO₂ is sensitive to biological processes in the high latitudes, e.g., in the North Pacific (McKinley et al., 2006), Southern Ocean (Metzl et al., 1999) and in the nutrient-rich low latitudes, i.e., the equatorial Pacific (Chai et al, 2002).

This study, applying the adjoint model, also presents the first comprehensive maps for the sensitivity of the global sea-to-air CO₂ flux to regional perturbations in nutrients and marine ecosystem model parameters. In regions where nutrients are the limiting factor, nutrient addition increases carbon fixation and will increase the uptake of atmospheric CO₂. However, this study shows that the amplitude of the outcome depends on the structure within the regional ecosystem. For example, in the equatorial Atlantic, the adjoint sensitivity maps illustrate that phosphate is an essential limiting factor because there is sufficient light, temperature, and iron as needed for phytoplankton growth. In addition, phosphate is highly depleted in these regions because nitrogen requirements are met by nitrogen fixation of cyanobacteria.

The global sea-to-air CO₂ flux is sensitive to changes in ecosystem parameters in regions with high annual-mean productivity, including the equatorial Pacific, the western part of North Pacific gyre, the North Atlantic, and the Southern Ocean. In all these regions, the sensitivity maps reveal high sensitivities to changes in zooplankton dynamics, specifically grazing and excretion parameters. An increase in zooplankton grazing would reduce the phytoplankton concentration and reduce DIC uptake because there would then be fewer phytoplankton to perform photosynthesis. In contrast, increasing zooplankton excretion rate would reduce zooplankton abundance and increase DOC concentration, both of which facilitate phytoplankton growth and enhance the upward flux of remineralized nutrient. Both changes also help maintain a longer phytoplankton growth period. Our adjoint sensitivity study suggests that increases phytoplankton growth rate increases the carbon uptake in the equatorial and northwest Pacific. In the oligotrophic regions (e.g., subtropical North and South Pacific), an increase in the exudation rate increases the dissolved organic carbon (DOC) surface concentrations. Therefore, over longer time scales, increased exudation would enhance regenerated nutrients, which would increase photosynthesis and carbon uptake.

Nevertheless, it is unlikely that a climate-associated change in one parameter does not affect or feedback on

other ecosystem processes or parameters. For example, Bopp et al. (2005) demonstrated that the diatom growing season in the high latitudes could potentially increase with global warming. Furthermore, increases in the stratification from climate change may also lead to the broadening of oligotrophic areas, which could increase smaller-sized phytoplankton stock and reduce POC sinking speed, thus the overall biological pump and carbon uptake. On the other hand, short-term manipulative experiments by Riebesell et al. (2007) suggest that phytoplankton carbon uptake may increase with rising oceanic CO₂ concentration, thereby resulting in higher organic carbon export. For the sensitivity of carbon uptake to regional nutrient addition, Aumont and Bopp (2006) demonstrated that local iron fertilization could alter the surface ecosystem dynamics and deep ocean biogeochemical tracer distribution, far from the fertilization sites.

Acknowledgements. We thank E. Maier-Reimer for providing the HAMOCC5 model and valuable discussions. We also thank T. Takahashi for providing the carbon flux data. We are very grateful to J. Orr for his thorough review and valuable feedback, which improve the overall quality of the manuscript. We also thank anonymous reviewers, and T. Sykes for their critical feedbacks. This research at the University of Wisconsin Center for Climatic Research was supported by the NASA (NAG-11245), the EU NOCES project (ENK2-CT-2001-00134), and the JGOFS (03F0321E). Arne Winguth is supported by NSF-EAR (0628336). Center for Climatic Research contribution 939.

Edited by: J. Orr

References

- Amon, R. H., W. and Benner, R.: Rapid cycling of high molecular weight dissolved organic matter in the ocean, *Nature*, 369, 549–552, 1994.
- Aumont, O., Maier-Reimer, E., Blain, S., and Monfray, P.: An ecosystem model of the global ocean including Fe, Si, P colimitations, *Global Biogeochem. Cy.*, 17, 1060, doi:10.1029/2001GB001745, 2003.
- Aumont, O. and Bopp, L.: Globalizing results from ocean in situ iron fertilization studies, *Global Biogeochem. Cy.*, 20, GB2017, doi:10.1029/2005GB002591, 2006.
- Berman-Frank, I., Cullen, J. T., Shaked, Y., Sherrell, R. M., and Falkowski, P. G.: Iron availability, cellular iron quotas, and nitrogen fixation in *Trichodesmium*, *Limnol. Oceanogr.* 46, 1249–1260, 2001.
- Bopp, L., Monfray, P., Aumont, O., Dufresne, J.-L., Treut, H. L., Madec, G., Terray, L., and Orr, J. C.: Potential impact of climate change on marine export production, *Global Biogeochem. Cy.*, 15, 81–99, 2001.
- Bopp, L., Kohfeld, K. E., Le Quéré, C., and Aumont, O.: Dust impact on marine biota and atmospheric CO₂, *Paleoceanography*, 18, 1046, doi:10.1029/2002PA000810, 2003.
- Bopp, L., Aumont, O., Cadule, P., Alvain, S., and Gehlen, M.: Response of diatoms distribution to global warming and potential implications: A global model study, *Geophys. Res. Lett.*, 32, L19606, doi:10.1029/2005GL023653, 2005.
- Boyd, P. W., Wong, C. S., Merrill, J., Whitney, F., Snow, J., Harrison, P. J., and Gower, J.: Atmospheric iron supply and enhanced vertical carbon flux in the NE subarctic Pacific: Is there a connection?, *Global Biogeochem. Cy.*, 12, 429–441, 1998.
- Boyd, P. W. and Doney, S. C.: Modelling regional response by marine pelagic ecosystems to global climate change, *Geophys. Res. Lett.*, 29(16), 53-1–53-4, doi:10.1029/2001GL014130, 2002.
- Carpenter, S. R., Cole, J. J., Hodgson, J. R., Kitchell, J. F., Pace, M. L., Bade, D., Cottingham, K. L., Essington, T. E., Houser, J. N., and Schindler, D. E.: Trophic Cascades, Nutrients, and Lake Productivity: Whole-Lake Experiments, *Ecological Monograph*, 71, 163–186, 2001.
- Chai, F., Dugdale, R. C., Peng, T. -H., Wilkerson, F. P., and Barber, R. T.: One-dimensional ecosystem model of the equatorial Pacific upwelling system. Part I: model development and silicon and nitrogen cycle, *Deep-Sea Res. II*, 49, 2713–2745, 2002.
- Chierici, M., Fransson, A., and Nojiri, Y.: Biogeochemical processes as drivers of surface fCO₂ in contrasting provinces in the subarctic North Pacific Ocean, *Global Biogeochem. Cycles*, 20, GB1009, doi:10.1029/2004GB002356, 2006.
- Conkright, M., Garcia, H. E., O'Brien, T. D., et al.: *World Ocean Atlas 2001*, vol. 4, Nutrients, NOAA Atlas NESDIS 6, NOAA, Silver Spring, Maryland, USA, 2002.
- Cox, P. M., Betts, R. A., Jones, C. D., Spall, S. A., and Totterdell, I. J.: Acceleration of global warming due to carbon-cycle feedbacks in a coupled climate model, *Nature*, 409, 184–187, 2000.
- de Baar, H. J. W., De Jong, J. T. M., Bakker, D. C. E., Löscher, B. M., Veth, C., Bathmann, U., and Smetacek, V.: Importance of iron for phytoplankton blooms and carbon dioxide drawdown in the Southern Ocean, *Nature*, 373, 412–415, 1995.
- Denman, K. L. and Pena, M. A.: The response of two coupled 1-D mixed layer/planktonic ecosystem models to climate change in the NE Subarctic Pacific Ocean, *Deep-Sea Res. II*, 49, 5739–5757, 2002.
- Doney, S. C., Lindsay, K., Caldeira, K., et al.: Evaluating global ocean carbon models: The importance of realistic physics, *Global Biogeochem. Cy.*, 18, GB3017, doi:10.1029/2003GB002150, 2004.
- Druon, J.-N. and Le Fevre, J.: Sensitivity of a pelagic ecosystem model to variations of process parameters within a realistic range, *J. Mar. Sys.*, 19, 1–26, 1999.
- Dugdale, R. C., Barber, R. T., Chai, F., Peng, T. -H., and Wilkerson, F. P.: One-dimensional ecosystem model of the equatorial Pacific upwelling system. Part II: sensitivity analysis and comparison with JGOFS EqPac data, *Deep-Sea Res. Part II*, 49, 2747–2768, 2002.
- Dutkiewicz, S., Follows, M. J., Heimbach, P., and Marshall, J.: Controls on ocean productivity and sea-to-air carbon flux: an adjoint model sensitivity study, *Geophys. Res. Lett.*, 33, L02603, doi:10.1029/2005GL024987, 2006.
- Enting, I. G., Wigley, T. M. L., and Heimann, M.: Future emissions and concentrations of carbon dioxide: Key ocean/atmosphere/land analysis, *Tech. Pap. 31*, Div. of Atmos. Res., Commonw. Sci. and Ind. Res. Org., Melbourne, Victoria, Australia, 1994.
- Eppley, R. W.: Temperature and phytoplankton growth in the sea, *Fish. Bull.*, 70, 1063–1085, 1972.

- Falkowski, P., Scholes, R. J., Boyle, E., Canadell, J., Canfield, D., Elser, J., Gruber, N., Hibbard, K., Hogbeg, P., Linder, S., MacKenzie, S. F., Moore III, B., Pedersen, T. F., Rosenthal, Y., Seitzinger, S., Smetacek, V., and Steffen, W.: The global carbon cycle: a test of our knowledge of Earth as a system, *Science*, 290, 291–296, 2002.
- FAO, Current world fertilizer trends and outlook to 2011/12, Food and Agriculture Organization of the United Nations (<http://www.fao.org/newsroom/en/news/2008/1000792/index.html>), Rome, 2008.
- Feely, R. A., Takahashi, T., Wanninkhof, R., McPhaden, M. J., Cosca, C. E., Sutherland, S. C., and Carr, M. E.: Decadal variability of the sea-to-air CO₂ fluxes in the equatorial Pacific Ocean, *J. Geophys. Res.*, 111, C08S90, doi:10.1029/2005JC003129, 2006.
- Friedlingstein, P., Cox, P., Betts, R., et al., Climate-carbon cycle feedback analysis: Results from the C4MIP model intercomparison, *J. Clim.*, 19, 3337–3353, 2006.
- Fung, I. Y., Doney, S. C., Lindsay, K., and John, J.: Evolution of carbon sinks in a changing climate, *Proc. Natl. Acad. Sci. USA*, 102, 11 201–11 206, 2005.
- Gehlen, M., Heinze, C., Maier-Reimer, E., and Measures, C. I.: Coupled Al-Si geochemistry in an ocean general circulation model: A tool for the validation of oceanic dust deposition fields?, *Global Biogeochem. Cy.*, 17, 1028, doi:10.1029/2001GB001549, 2003.
- Giering, R.: Assimilation von satellitendaten in ein dreidimensionales numerisches Modell der atlantischen Zirkulation, M. S. thesis, Univ. of Hamburg, Hamburg, Germany, 1989.
- Giering, R. and Kaminski, T.: Recipes for adjoint code construction, *ACM Transactions on Mathematical Software*, 24, 437–474, 1998.
- Gloor, M., Gruber, N., Sarmiento, J., Sabine, C. L., Feely, R. A., and Rödenbeck, C.: A first estimate of present and preindustrial sea-to-air CO₂ flux patterns based on ocean interior carbon measurements and models, *Geophys. Res. Lett.*, 30, 1010, doi:10.1029/2002GL015594, 2003.
- Gnanadesikan, A., Sarmiento, J. L., and Slater, R. D.: Effects of patchy ocean fertilization on atmospheric carbon dioxide and biological production, *Global Biogeochem. Cy.*, 17, 1050, doi:10.1029/2002GB001940, 2003.
- Heinze, C., Maier-Reimer, E., Winguth, A. M. E., and Archer, D.: A global oceanic sediment model for long-term climate studies, *Glob. Biogeochem. Cy.*, 13, 221–250, 1999.
- Hoffmann, L.: Marine cyanobacteria in tropical regions: diversity and ecology, *Eur. J. Phycol.*, 34, 371–379, 1999.
- Hood, R. R., Laws, E. A., Armstrong, R. A., et al.: Pelagic functional group modeling: Progress, challenges, and prospects, *Deep-Sea Res. Part II*, 53, 459–512, 2006.
- Howard, M. T., Winguth, A. M. E., Klaas, C., and Maier-Reimer, E.: Sensitivity of ocean carbon tracer distributions to particulate organic flux parameterizations, *Global Biogeochem. Cy.*, 20, GB3011, doi:10.1029/2005GB002499, 2006.
- Karl, D. M., Hebel, D. V., and Tupas, L. M.: Biogeochemical studies at the Hawaii Ocean Time-series (HOT) station ALOHA, Joint GCOS GOOS WCRP Ocean Observations Panel for Climate (OOPC), GCOS Report No. 41, 1997.
- Landry, M. R., Selph, K. E., Brown, S. L., Abbott, M. R., Measures, C. I., Vink, S., Allen, C. B., Calbet, A., Christensen, S., and Nolla, H.: Seasonal dynamics of phytoplankton in the Antarctic Polar Front regions at 170° W, *Deep-Sea Res. Part II*, 49, 1843–1865, 2002.
- Landry, M. R., Brown, S. L., Neveux, J., Dupouy, C., et al.: Phytoplankton growth and microzooplankton grazing in high-nutrient, low-chlorophyll waters of the equatorial Pacific: Community and taxon-specific rate assessments from pigment and flow cytometric analyses, *J. Geophys. Res.*, 108(C12), 8142, doi:10.1029/2000JC000744, 2003.
- Le Quéré, C., Orr, J. C., Monfray, P., Aumont, O., and Madec, G.: Interannual variability of the oceanic sink of CO₂ from 1979 through 1997, *Global Biogeochem. Cy.*, 14, 1247–1265, 2000.
- Le Quéré, C., Harrison, S. P., Colin Prentice, I., et al., Ecosystem dynamics based on plankton functional types for global ocean biogeochemistry models, *Glob. Change Biol.*, 11, 2016–2040, doi:10.1111/j.1365-2486.2005.01004.x, 2005.
- Lessard, E. J. and Murrell, M. C.: Microzooplankton herbivory and phytoplankton growth in the northwestern Sargasso Sea, *Aquatic Microbial Ecology*, 16, 173–188, 1998.
- Maier-Reimer, E., Geochemical cycles in an ocean general circulation model. Preindustrial tracer distributions, *Global Biogeochem. Cy.*, 7, 645–677, 1993.
- Maier-Reimer, E., Mikolajewicz, U., and Hasselmann, K.: Mean circulation of the Hamburg LSG OGCM and its sensitivity to the thermohaline surface forcing, *J. Phys. Oceanogr.*, 23, 731–757, 1993.
- Maier-Reimer, E., Mikolajewicz, U., and Winguth, A.: Future ocean uptake of CO₂ - Interaction between ocean circulation and biology, *Clim. Dynam.*, 12, 711–721, 1996.
- Maier-Reimer, E., Kriest, I., Segschneider, J., and Wetzel, P.: The Hamburg Ocean Carbon Cycle model HAMOCC 5.1, Technical description release 1.1, Reports on Earth System Science, Max Planck Institute for Meteorology, Hamburg, Germany, 2005.
- Manizza, M., Le Quéré, C., Watson, A. J., Buitenhuis, E. T.: Bio-optical feedbacks among phytoplankton, upper ocean physics and sea-ice in a global model, *Geophys. Res. Lett.*, 32, L05603, doi:10.1029/2004GL020778, 2005.
- Matear, R. J. and Hirst, A. C.: Climate change feedback on the future oceanic CO₂ uptake, *Tellus Ser. B-Chem. Phys. Meteorol.*, 51, 722–733, 1999.
- McKinley, G. A., Follows, M. J., and Marshall, J.: Mechanism of sea-to-air CO₂ flux variability in the equatorial Pacific and the North Atlantic, *Global Biogeochem. Cy.*, 18, GB2011, doi:10.1029/2003GB002179, 2004.
- McKinley, G. A., Takahashi, T., Buitenhuis, E., et al.: North Pacific carbon cycle response to climate variability on seasonal to decadal timescales. *J. Geophys. Res.*, 111, C07S06, doi:10.1029/2005JC00317, 2006.
- Metzl, N., Tilbrook, B., and Poisson, A.: The annual fCO₂ cycle and the sea-to-air CO₂ flux in the sub-Antarctic Ocean, *Tellus*, B 51, 849–861, 1999.
- Mikolajewicz, U., Groger, M., Maier-Reimer, E., Schurgers, G., Vizza, M., and Winguth, A. M. E.: Long-term effects of anthropogenic CO₂ emissions simulated with a complex earth system model, *Clim. Dynam.*, 28(6), 599–633, doi: 10.1007/s00382-006-0204-y, 2007.
- Moore, J. K., Doney, S. C., Kleypas, J. A., Glover, D. M., and Fung, I. Y.: An intermediate complexity marine ecosystem model for the global domain, *Deep-Sea Res. Part II*, 49, 403–462, 2002.

- Moore, J. K., Doney, S. C., and Lindsay, K.: Upper ocean ecosystem dynamics and iron cycling in a global three-dimensional model, *Global Biogeochem. Cy.*, 18, GB4028, doi:10.1029/2004GB002220, 2004.
- Olsen, A., Brown, K. R., Chierici, M., Johanessen, T., and Neils, C.: The sea-surface CO₂ fugacity in the subpolar North Atlantic 2005, *Biogeosciences Discuss.*, 4, 1737–1777, 2007, <http://www.biogeosciences-discuss.net/4/1737/2007/>.
- Oschlies, A., and Kähler, P., Biotic contribution to sea-to-air fluxes of CO₂ and O₂ and its relation to new production, export production, and net community production, *Global Biogeochem. Cy.*, 18, GB1015, doi:10.1029/2003GB002094, 2004.
- Parekh, P., Follows, M. J., and Boyle, E. A.: Decoupling of iron and phosphate in the global ocean, *Global Biogeochem. Cy.*, 19, GB2020, doi:10.1029/2004GB002280, 2005.
- Parekh, P., Dutkiewicz, S., Follows, M., and Ito, T.: Atmospheric carbon dioxide in a less dusty world, *Geophys. Res. Lett.*, 33, L03610, doi:10.1029/2005GL025098, 2006.
- Pasquer, T., Laruelle, G., Becquevort, S., Schoemann, V., Goosse, H., and Lancelot, C.: Linking ocean biogeochemical cycles and ecosystem structure and function: results of the complex SWAMCO-4 model, *J. Sea Res.*, 53, 93–108, 2005.
- Plattner, G.-K., Joos, F., Stocker, T. F., and Marchal, O.: Feedback mechanisms and sensitivities of ocean carbon uptake under global warming, *Tellus, Ser. B*, 53, 564–592, 2001.
- Popova, E. E., Coward, A. C., Nurser, G. A., de Cuevas, B., Fasham, M. J. R., and Anderson, T. R.: Mechanisms controlling primary and new production in a global ecosystem model – Part I: Validation of the biological simulation, *Ocean Sci.*, 2, 249–266, 2006, <http://www.ocean-sci.net/2/249/2006/>.
- Price, N. M., Ahner, B. A., and Morel, F. M. M.: The equatorial Pacific Ocean: Grazer-controlled phytoplankton populations in an iron-limited ecosystem, *Limnol. Oceanogr.*, 39, 520–534, 1994.
- Richardson, K., Visser, A. W., and Pederson, F. Bo.: Subsurface phytoplankton blooms fuel pelagic production in the North Sea, *J. Plank. Res.* 22, 1663–1671, 2000.
- Riebesell, U., Schulz, K. G., Bellerby, R. G. J., Botros, M., Fritsche, P., Meyerhöfer, M., Neill, C., Nondal, G., Oschlies, A., Wohlers, J., and Zöllner, E., Enhanced biological carbon consumption in high CO₂ ocean, *Nature*, 450, 545–548, 2007.
- Sabine, C. L., Feely, R. A., Johnson, G. C., Strutton, P. G., Lamb, M. F., and McTaggart, K. E., A mixed layer carbon budget for the GasEx-2001 experiment, *J. Geophys. Res.*, 109, C08S05, doi:10.1029/2002JC001747, 2004.
- Saito, H., Suzuki, K., Hinuma, A., Ota, T., Fukami, K., Kiyosawa, H., Saino, T., and Tsuda, A., Responses of microzooplankton to in situ iron fertilization in the western Subarctic Pacific (SEEDS), *Progress in Oceanogr.*, 64(2–4), 223–236, 2005.
- Sarma, V. V. S. S., Swathi, P. S., Dileep Kumar, M., Prasannakumar, S., Bhattathiri, P. M. A., Madhupratap, M., Ramaswamy, V., Sarin, M. M., Gauns, M., Ramaiah, M., Sardesai, S., and de Sousa, S. N.: Carbon budget in the eastern and central Arabian Sea: An Indian JGOFS synthesis, *Global Biogeochem. Cy.*, 17, 1102, doi:10.1029/2002GB001978, 2003.
- Sarmiento, J. L. and Orr, J. C., Three-dimensional simulation of the impact of southern ocean nutrient depletion on atmospheric CO₂ and ocean chemistry, *Limnol. Oceanogr.*, 36, 1928–1950, 1991.
- Sarmiento, J. L., Hughes, T. M. C., Stouffer, R. J., and Manabe, S.: Simulated response of the ocean carbon cycle to anthropogenic climate warming, *Nature*, 393(6682), 245–249, 1998.
- Schindler, D. E., Carpenter, S. R., Cole, J. J., Kitchell, J. F., and Pace, M. L.: Influence of Food Web Structure on Carbon Exchange Between Lakes and the Atmosphere, *Science*, 227, 248–251, 1997.
- Schrum, C., Alekseeva, I., John, M. S.: Development of a coupled physical-biological ecosystem model ECOSMO Part I: Model description and validation for the North Sea, *J. Mar. Sys.*, in press, 2008.
- Six, K. D. and Maier-Reimer, E.: Effects of plankton dynamics on seasonal carbon fluxes in an ocean general circulation model, *Global Biogeochem. Cy.*, 10, 559–583, 1996.
- Smetacek, V.: A watery arms race, *Nature*, 14, 745, 2001.
- Takahashi, T., Olafsson, J., Goddard, J. G., Chipman, D. W., and Sutherland, S. C.: Seasonal variation of CO₂ and nutrients in the highlatitude surface oceans: A comparative study, *Global Biogeochem. Cy.*, 7, 843–878, 1993.
- Takahashi, T., Sutherland, M. L., Sweeney, C., Poisson, A., Metzel, N., Tilbrook, B., Bates, N., Wanninkhof, R., Feely, R. A., Sabine, C., Olafsson, J., and Nojiri, Y.: Global sea-air CO₂ flux based on climatological surface ocean pCO₂, and seasonal biological and temperature effects, *Deep-Sea Res. II*, 49, 1601–1622, 2002.
- Tjiputra, J.: Analysis of marine ecosystem dynamics using an adjoint three-dimensional ocean carbon cycle model, Ph.D. Dissertation, University of Wisconsin, USA, 2007.
- Tjiputra, J. F., Polzin, D., and Winguth, A. M. E.: Assimilation of seasonal chlorophyll and nutrient data into an adjoint three-dimensional ocean carbon cycle model: Sensitivity analysis and ecosystem parameter optimization, *Global Biogeochem. Cy.*, 21, GB1001, doi:10.1029/2006GB002745, 2007.
- Tyrrell, T.: The relative influences of nitrogen and phosphorus on oceanic primary production, *Nature*, 400, 525–531, 1999.
- Volk, T. and Hoffert, M. I.: Ocean carbon pumps: Analysis of relative strengths and efficiencies in ocean-driven atmospheric CO₂ changes, in: *The Carbon Cycle and Atmospheric CO₂: Natural Variations Archaean to Present*, edited by: E. T. Sunquist and W. S. Broecker, 99–110, AGU, Washington, D. C., 1985.
- Völker, C. and Wallace, D. W. R., On the role of heat fluxes in the uptake of anthropogenic carbon in the North Atlantic, *Global Biogeochem. Cy.*, 16(4), 1138, doi:10.1029/2002GB001897, 2002.
- Wang, X., Christian, J. R., Murtugudde, R., and Busalacchi, J.: Spatial and temporal variability of the surface water pCO₂ and air sea CO₂ flux in the equatorial Pacific during 1980–2003: A basin-scale carbon cycle model, *J. Geophys. Res.*, 111, C07S04, doi:10.1029/2005JC002972, 2006.
- Wanninkhof, R.: Relationship between wind speed and gas exchange over the ocean, *J. Geophys. Res.*, 97, 7373–7382, 1992.
- Watson, A. J. and Orr, J. C.: Carbon dioxide fluxes in the global ocean, in: *Ocean Biogeochemistry. The role of the ocean carbon cycle in global change*, edited by: M. J. R. Fasham, 123–143, Springer-Verlag, Berlin, 2003.
- Weiss, R. F.: Carbon dioxide in water and seawater: The solubility of a non-ideal gas, *Marine Chemistry*, 2, 203–215, 1974.
- Wetzel, P.: Interannual and decadal variability in the sea-to-air exchange of CO₂ – a model study, Report on Earth System Science (Ph.D. Dissertation), Max-Planck-Institut für Meteorologie, Hamburg, Germany, 2004.
- Wetzel, P., Winguth, A., and Maier-Reimer, E.: Sea-to-air CO₂ flux

- from 1948 to 2003: A model study, *Global Biogeochem. Cy.*, 19, GB2005, doi:10.1029/2004GB002339, 2005.
- Winguth, A., Mikolajewicz, U., Groger, M., Maier-Reimer, E., Schurgers, G., and Vizcano, M.: Centennial-scale interactions between the carbon cycle and anthropogenic climate change using a dynamic Earth system model, *Geophys. Res. Lett.*, 32, L23714, doi:10.1029/2005GL023681, 2005.
- Wrona, F. J., Prowse, T. D., Reist, J. D., Hobbie, J. E., Lévesque, L. M. J., and Vincent, W. F.: Climate change effects on aquatic biota, ecosystem structure and function, *AMBIO: A Journal of the Human Environment*, 35, 347–358, 2006.
- Wu, J. F., Sunda, W., Boyle, E. A., and Karl, D. M.: Phosphate depletion in the western North Atlantic Ocean, *Science*, 239, 759–762, 2000.
- Zeebe, R. E. and Archer, D.: Feasibility of ocean fertilization and its impacts on future atmospheric CO₂ levels, *Geophys. Res. Lett.*, 32, L09703, doi:10.1029/2005GL022449, 2005.
- Zhao, L., Wei, H., Xu, Y., and Feng, S.: An adjoint data assimilation approach for estimating parameters in a three-dimensional ecosystem model, *Ecological Modelling*, 186, 234–249, 2005.